REVISTA INTERDISCIPLINAR DE PESQUISA EM ENGENHARIA

CILAMCE 2016

XXXVII IBERIAN LATIN AMERICAN CONGRESS
ON COMPUTATIONAL METHODS IN ENGINEERING
BRASÍLIA - DF - BRAZIL

GENETIC OPTIMIZATION ANALYSIS OF WIND TOWER VIBRATIONS CONTROLLED BY A PENDULUM TMD

Gino Bertollucci Colherinhas; **Marcus Vinicius Girão de Morais**

ginobertollucci@hotmal.com; mvmorais@unb.br

Universidade de Brasília - Faculdade de Tecnologia

Campus Universitário Darcy Ribeiro, Asa Norte - 70.910-900, Brasília, DF, BRAZIL

Maura Angélica Milfont Shzu; **Suzana Moreira Ávila**

maura@unb.br; avilas@unb.br

Universidade de Brasília - Faculdade UnB-Gama

Campus UnB Gama, Área Especial Indústria e Projeção A - 72.444-240, Gama, DF, BRAZIL

Abstract. *The wind turbine is supported by towers, which are slender and flexible due to their geometry and great height. As a consequence, they may experience excessive vibration levels caused by both the operation of the turbine and the wind loads. One common passive control device to solve this problem is the Tuned Mass Damper (TMD). Briefly, it is a pendulum-damper which transfers the energy of the vibration from the main structure to itself, working as a passive device. These passive devices need to be finely tuned to work as dampers, otherwise, they could amplify structural vibrations levels. The objective of this paper was create a project methodology to optimize a pendulum + mass-spring (2-DoF) structural model. The mass, length, stiffness, and damping coefficient of the pendulum were the parameters surveyed for this optimization. We carry out a map of high vibration amplitudes describing the dynamic behavior of the 2-DoF structural model. This map was used to validate 2-DoF's GA optimization results. Then we compared the finite element models (BEAM and SHELL) obtained integrating the commercial platform ANSYS with the MATLAB toolbox. A project methodology was reached to define optimum absorber configurations.*

Keywords: *Wind Turbine, Tuned Mass Damper, Algorithm Optimization, Structural Control*

1 Introduction

The current energy crises coupled to the depletion of fossil fuel stocks and the need to reduce emissions of carbonic gas, in order to preserve the environment makes wind power generation a viable and attractive mean for producing electricity.

The wind turbine is supported by a tower that can experience excessive vibrations caused by both the wind turbine and the wind forces because of its geometry and great height. A detailed analysis of the structural behavior of the tower is of great importance due to its cost, which can represent approximately 20% of the total cost of the system (Morais et al., 2009).

Given the great progress in analyses and structural dimensioning, with the advances in the material field and construction techniques, higher and slender structures have become more interesting to study. These structures, however, are more vulnerable to excessive vibrations due to dynamic loads such as earthquakes, winds, storms, waves, etc.

An alternative option widely studied in the last few years is the structural control. It is classified as passive, active, hybrid, or semi-active control. Several researchers have been studying the use of structural control to help suppress the wind-induced vibrations experienced by wind turbine towers (Nigdeli & Bekdaş, 2016; Avila et al., 2016; Stewart & Lackner, 2014; Lackner & Rotea, 2011).

To minimize these vibrations, we implemented a structural control with a Tuned Mass Damper (TMD) Pendulum type. A TMD is a passive control device composed of a mass-spring-dashpot attached to the structure, aiming to reduce structural vibration response (Soong & Dargush, 1997). A newest version of a developed GA toolbox (Colherinhas et al., 2015b,a) was used to achieve the optimization.

The aim of this article is create a project methodology to assist wind turbine design projects, enabling the selection of an optimum pendulum configuration that targets a minimization of the frequency peaks. The pendulum parameters surveyed are: stiffness, damping, length and mass. After the selection of the parameters, we approach the mathematical model to the numerical.

The tower was modeled via finite element method (FEM) using beam and shell elements (Avila et al., 2009; Shzu et al., 2015). The natural frequencies and the mode shapes of the models were obtained as well as transient and harmonic analysis results to determine the dynamic response of the tower in time domain, considering wind loads.

Although structural control of slender and great height towers using pendulum TMDs is widely studied in literature, studies modeling the pendulum TMD with ANSYS it wasn't found yet. This is a potential tool to study the performance of this system attached to excessive vibration vulnerable structures like wind turbines.

Depending on the result obtained for the evaluation of this modeling, fitness is ascribed to each configuration and inputted in a Genetic Algorithm (GA) to optimize the initial pendulum values for mass and length. This optimization method was chosen for its advantages at discontinuous functions with multiple variables and complex formulations.

The following sections describes the Analytical 2-DoF model of a wind turbine tower + Pendulum TMD, the sensibility analysis (response maps), the optimization method chosen (definitions of the chromosome, fitness function, and convergence criteria), and the project methodology.

2 Analitical model

This section presents a reduced dynamic model for the slender tower, later the TMD effects are added. At firs the tower is looked upon a 1-DoF approach, so the couplet system tower+TMD is approximated as two degrees of freedom.

The motion of a cantilever Bernoulli-Euler beam, shown in Fig. 1, can be described as:

$$\frac{\partial^2}{\partial z^2}\left(EI\frac{\partial^2 w(z,t)}{\partial z^2}\right)+\rho\frac{\partial^2 w(z,t)}{\partial t^2}=F(z,t) \tag{1}$$

where $w(z,t)$ is the normal displacement, z the position along the beam axis, ρ the mass per length unit of the beam, F the external force per length unit applied in w direction, E the Young Modulus, I second moment of area for bending.

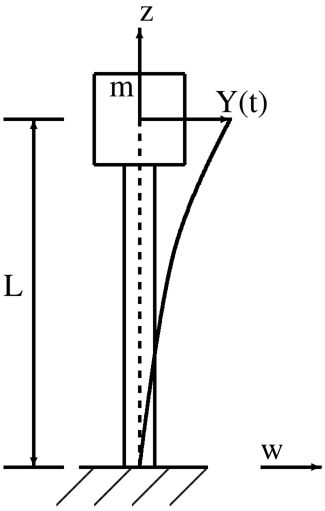

Figure 1: Description of a cantilever beam with a tip mass m

The modal analysis reduce the complex system of partial differential equation which describes the dynamic behavior of a continuous structure. A theoretical approach to modal analysis is observed at Meirovitch (1967); Morais et al. (2009).

2.1 Order reduction

Applying boundary conditions and solving the partial differential equation (Ávila et al., 2009) the generalized stiffness and mass of the tower are computed, respectively in Eqs. 2 and 3.

$$K_s=\frac{\pi^4}{32L^3}EI \tag{2}$$

$$M_s=\frac{mL}{2\pi}\left[\pi\left(3+2\frac{L_e}{L}\right)-8\right] \tag{3}$$

where the tip mass $M_s=mL_e$ is defined proportional as an equivalent length L_e.

2.2 Analytical 2-DoF - Pendulum TMD + Tower

With the main system reduced to a 1-DoF model, which corresponds to the mode to be controlled (Soong & Dargush, 1997), the dynamic behavior of a Pendulum TMD is coupled. This gives a 2-DoF discrete system described by the Fig. 2.

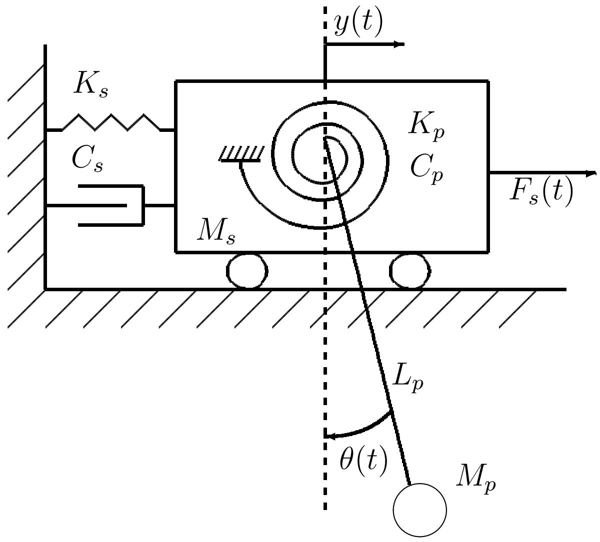

Figure 2: Structure with a linear pendulum attached excited by a force $F_s(t)$.

The motion considering small displacements is given by the matrix:

$$\begin{bmatrix} (M_s+M_p) & M_pL_p \\ M_pL_p & M_pL_p^2 \end{bmatrix} \begin{bmatrix} \ddot{y} \\ \ddot{\theta} \end{bmatrix} + \begin{bmatrix} C_s & 0 \\ 0 & C_p \end{bmatrix} \begin{bmatrix} \dot{y} \\ \dot{\theta} \end{bmatrix} + \begin{bmatrix} K_s & 0 \\ 0 & (K_p+M_pgL_p) \end{bmatrix} \begin{bmatrix} y \\ \theta \end{bmatrix} = \begin{bmatrix} F_s(t) \\ 0 \end{bmatrix} \tag{4}$$

where M_s: main system modal mass; C_s: main system modal damping; K_s: main system modal stiffness; M_p: pendulum mass; C_p: pendulum damping; K_p: pendulum stiffness; L: cable length; g: gravity acceleration; $F_s(t) = F_{s0}e^{i\omega t}$: excitation modal force; $y(t)$: main system displacement; $\theta(t)$: pendulum angular displacement.

Considering $F_s(t) = e^{i\omega t}$ and doing $y(t) = H_y(\omega)e^{i\omega t}$ and $\theta(t) = H_\theta(\omega)e^{i\omega t}$, we replace this considerations in Equation 4, obtaining the linear equation system:

$$\begin{bmatrix} -(M_s+M_p)\omega^2 + C_si\omega + K_s & -M_pL_p\omega^2 \\ -M_pL_p\omega^2 & -M_pL_p^2\omega^2 + C_pi\omega + (K_p+M_pgL_p) \end{bmatrix} \begin{bmatrix} H_y(\omega) \\ H_\theta(\omega) \end{bmatrix} = \begin{bmatrix} 1 \\ 0 \end{bmatrix} \tag{5}$$

where $H_y(\omega)$ is the structure response function in the frequency domain and $H_\theta(\omega)$ is the pendulum response function in the frequency domain.

Solving this linear equation system, Zuluaga (2007) obtained the response functions $H_y(\omega)$ and $H_\theta(\omega)$ in the frequency domain:

$$H_y(\omega) = \frac{A_{y0} + A_{y1}\omega + A_{y2}\omega^2}{B_0 + B_1\omega + B_2\omega^2 + B_3\omega^3 + B_4\omega^4} \tag{6}$$

$$H_\theta(\omega) = \frac{A_{\theta 0} + A_{\theta 1}\omega + A_{\theta 2}\omega^2}{B_0 + B_1\omega + B_2\omega^2 + B_3\omega^3 + B_4\omega^4} \tag{7}$$

where $A_{y0} = L_p M_p g + K_p$; $A_{y1} = iC_p L_p^2$; $A_{y2} = -L_p^2 M_p$; (Structure)

$A_{\theta 0} = 0$; $A_{\theta 1} = 0$; $A_{\theta 2} = L_p M_p$; (Pendulum)

$B_0 = K_s(K_p + L_p M_p g)$;

$B_1 = i(C_s K_p + C_p K_s L_p^2 + C_s L_p M_p g)$;

$B_2 = -(K_p M_p + K_p M_s + C_p C_s L_p^2 + K_s L_p^2 M_p + L_p M_p^2 g + L_p M_p M_s g)$;

$B_3 = -iL_p^2(C_p M_s + C_s M_p + C_p M_p)$;

$B_4 = L_p^2 M_p M_s$;

3 Sensibility analysis – response maps

The length L_p, mass M_p, damping C_p and stiffness K_p defines the pendulum configuration.

In order to study these variables sensibility an objective function is defined which evaluates each pendulum configuration through one single parameter. A great indicator of excessive vibration is it's frequencies response $H_y(\omega)$. Aiming to reduce frequency response peaks, the structure behavior is evaluated for different pendulum configurations.

We define response maps as the relation of the pendulum length L_p and mass ratio $\mu = M_p/M_s$ in function of the response peaks $max(H_y(\omega))$. These peaks contain the maximum values of the Frequency Response Functions (FRF) harmonic analysis of the combinations between L_p and μ.

The tower was constructed using steel ($E = 2,1.10^{11} N/m^2$, $\rho_{ao} = 7850 kg/m^3$) with height $H = 60m$, external diameter $d_e = 3m$, and thickness $e = 0,015m$. The tower carries the nacelle and rotor systems with $M_t = 19876kg$. This is a simple model with realistic dimensions of a tower, studied by Murtagh et al. (2004); Avila et al. (2009); Shzu et al. (2015)

Applying these considerations, the generalized stiffness and mass were obtained by Eqs. (2) and (3), giving $K_s = 463671,26 N/m$ and $M_s = 34899,6kg$, respectively. The tower damping was considered negligible $C_s \approx 0$. The mass, torsional stiffness, and damping of the pendulum are $M_p = 9198.6kg$, $K_p = 1247900N/m$, and $C_p = 9024,9Nms$, respectively.

Considering these design criteria the Figure 3 shows the response map. It's noticed a valley on this map. This geometric locus represents an optimal combination of the 2-GdL model.

The response map in the superior view (Fig. 4) shows clearly the curvilinear shape of the locus of optimal solutions. For the pendulum mass $M_p = 9198,6kg$, we makes up an appointment in response map at the point $L_p = 4m$ and $\mu = 0,26$ referring to the design values (Shzu et al., 2015).

Another appointment is realized in this figure considering the same mass ratio $\mu = 0,26$. Despite the solution for $L_p = 4,00m$ is'nt the optimal, the magnitude order is quite similar, as shown below:

For $L_p = 4,00$: $H_y(\omega) = e^{-8,804} = 1,51.10^{-4}m$.

For $L_p = 4,36$: $H_y(\omega) = e^{-9,057} = 1,16.10^{-4}m$.

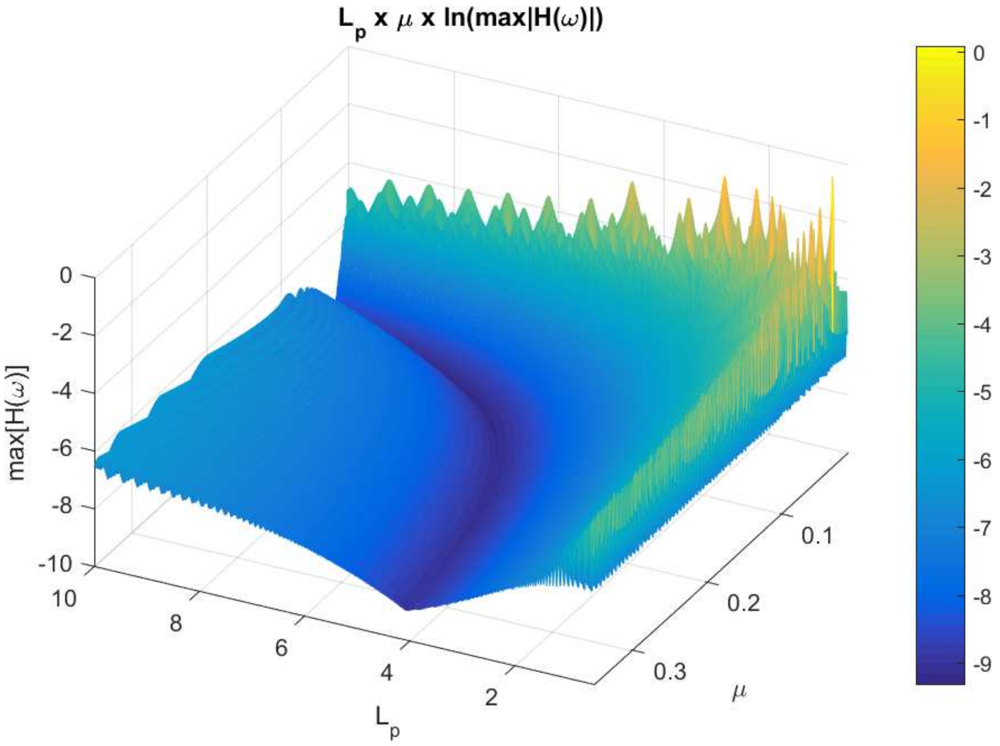

Figure 3: Response map - 3D view

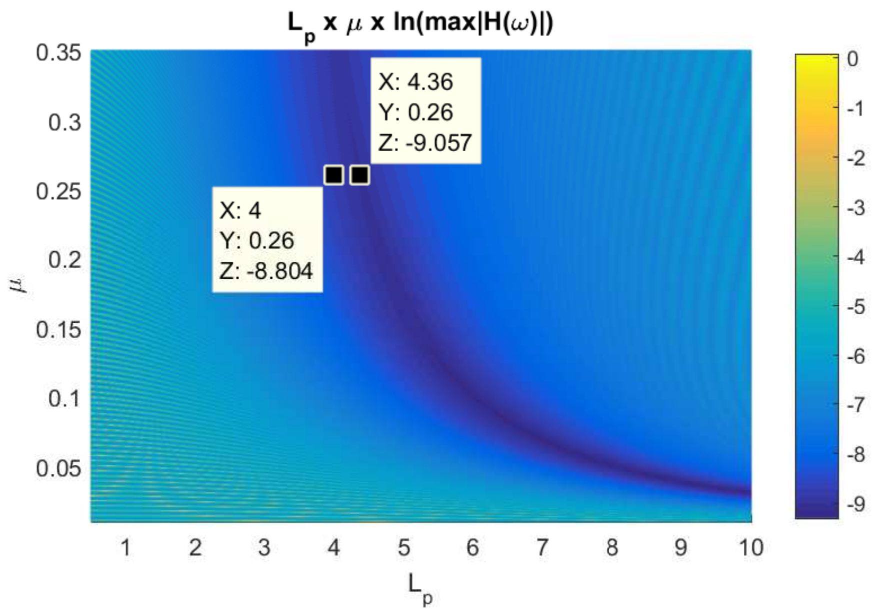

Figure 4: Response map - L_p vs μ view

3.1 Influences of damping C_p and stiffness K_p

To analyze the sensibility of the torsional damping over the dynamic effects of the structure, we analyzed two cases $C_p = \{5000, 15000\}Nms$, using the same stiffness ($K_p = 1247900N/m$). The relative curves obtained by the response maps has the same shape. However, the frequency response values were lower for larger damping.

For $C_p = 5000Nms$: $H_y(\omega) = e^{-8{,}461} = 1,12.10^{-4}m$.

For $C_p = 15000Nms$: $H_y(\omega) = e^{-9{,}556} = 7,08.10^{-5}m$.

This behavior extends for another values of C_p. The form and position of the curve on the response map remains unchanged in plan L_p vs. μ. The response amplitudes decreases as the damping increases.

For the torsional stiffness, the values $K_p = \{500000, 1000000, 1500000\}N/m$ are analyzed using the same damping ($C_p = 9024,9Nms$). It's concluded that the valley moves over the plan L_p vs. μ. When the stiffness K_p increases, the curve shifts to the right and the response values $H_y(\omega)$ increases too, as shown below:

For $K_p = 500000N/m$: $H_y(\omega) = e^{-9{,}803} = 5,53.10^{-5}m$.

For $K_p = 1000000N/m$: $H_y(\omega) = e^{-9{,}242} = 9,69.10^{-5}m$

For $K_p = 1500000N/m$: $H_y(\omega) = e^{-8{,}892} = 13,75.10^{-5}m$.

4 Genetic Algorithm Optimization (GA)

To assist the analysis of the response maps (Section 3), we elaborated a optimization methodology using the GA toolbox.

The parameters chosen for optimization were the pendulum length L_p and the mass ratio μ. The initial population $C = [L_p; \mu]$ is created restricting the variables in the following ranges:

$$\begin{aligned} 0.50 \le L_p \le 10.00 \\ 0.01 \le \mu \le 0.15 \end{aligned} \tag{8}$$

4.1 Fitness Function

The purpose of this optimization is to minimize the frequency response peaks of the the tower described in the Analytical 2-DoF formulation (Eq. 6). The fitness function minimizes $H_y(\omega)$ maximizing its inverse.

$$f_{obj} = \frac{1}{\max H_y(\omega)_i}, \text{ sendo } i = 1, 2, \ldots, N_{ind} \tag{9}$$

where i is the chromosome of the population N_{ind}.

4.2 Results

Defined the fitness function f_{obj}, the genetic toolbox uses the following parameters:

- $N_{ger} = 200$, number of generations;

- $N_{ind} = 200$, number of individuals in the population;
- $p_c = 60\%$, crossover probability;
- $p_m = 2\%$, mutation probability;
- $p_{elit} = 2\%$, elitism probability;
- $p_{diz} = 20\%$, decimation probability;
- $N_{diz} = 50$, step of generation for the occurence of decimation.

The optimum values for the optimization were $L_p = 7.08m$ and $\mu = 0,0663$. The peak response happens when $H(\omega) = 9,224 \cdot 10^{-5}\ m$ for the natural frequency $\omega = 0,509\ Hz$ (Fig. 5).

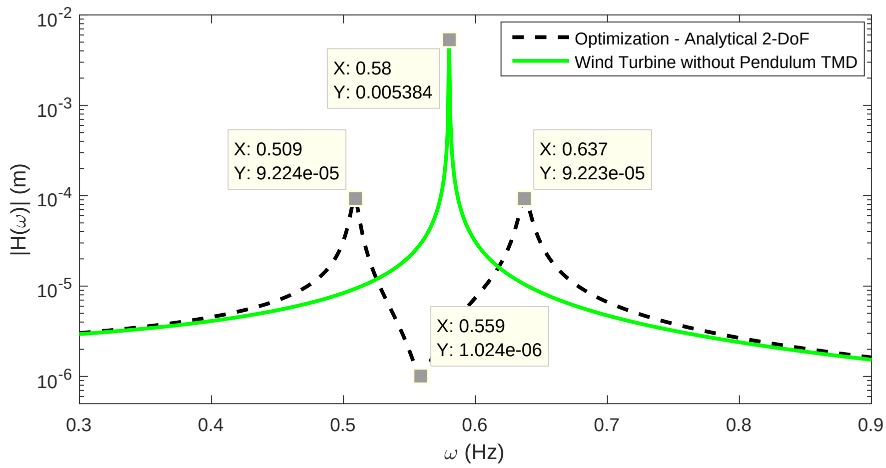

Figure 5: Frequency Response of the wind tower with and without the optimum Pendulum TMD

Another 300 optimizations have been made resulting in optimal solutions located close to the geometric locus in response map for various combinations of L_p and μ (Fig.6).

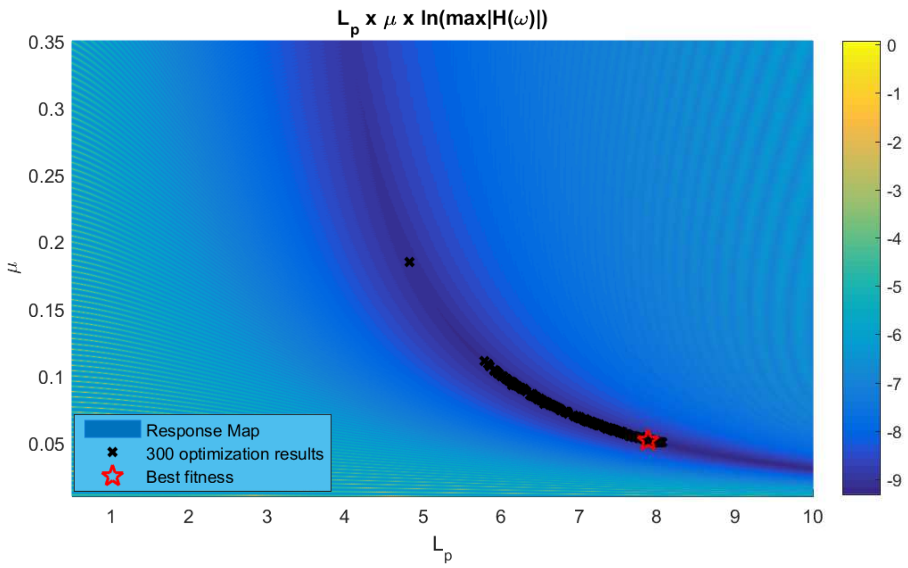

Figure 6: Optimum results (L_p,μ) compared to the response map

The optimization using the genetic toolbox works well and quickly for this fitness function. This feature defines the GAs as a versatile tool that can find different solutions to a engineering problem.

4.3 Results Analysis

A study over the results is carried out to estimate the appopriate regressions of the locus obtained by the response map.

For each value of $K_p = [0,25; 0,50; 0,75; 1,00; 1,25; 1,50; 1,75; 2,00] \cdot 10^6\ N/m$ 300 optimizations are performed. These points are arranged on a L_p vs. μ plan and their power regressions (Fig. 7) in $\mu = C_i L_p^{\alpha_i}$ form are showed.

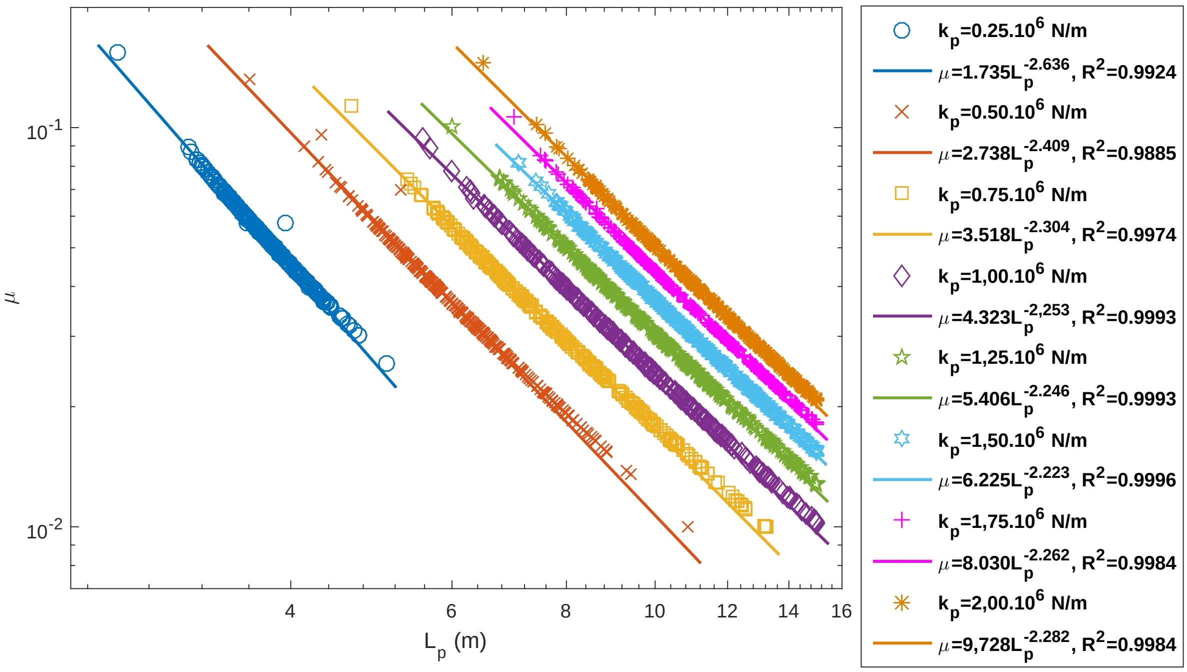

Figure 7: Power regression of $(\mu; L_p)$ over the optimization results

These power functions presents a certain linearity in *log-log* scale. These relationships are important for the designer who wants to project pendulum parameters, since the damping C_p does not affect the behavior of these curves.

5 Finite Element Method (FEM)

Aiming to approximate the 2-DoF to realistic models, structural systems spring-mass+pendulum (2-DoF), beam+pendulum, and shell+pendulum are modeled using the software *ANSYS Mechanical APDL* (Avila et al., 2016; Shzu et al., 2015). These three numerical models are compared to the 2-DoF Analytical in Figure 8 for three lengths $L_p = [2, 4, 6]m$.

When the pendulum length L_p increases, the response $H_y(\omega)$ decreases for the first mode, while the second mode increases. With the increase of the L_p the FRF curve moves to the left.

Figure 8 shows similar FRFs characteristics between the 2-DoF and BEAM models with relative error values near 4%. This difference is greater between the 2-DoF and FEM Shell

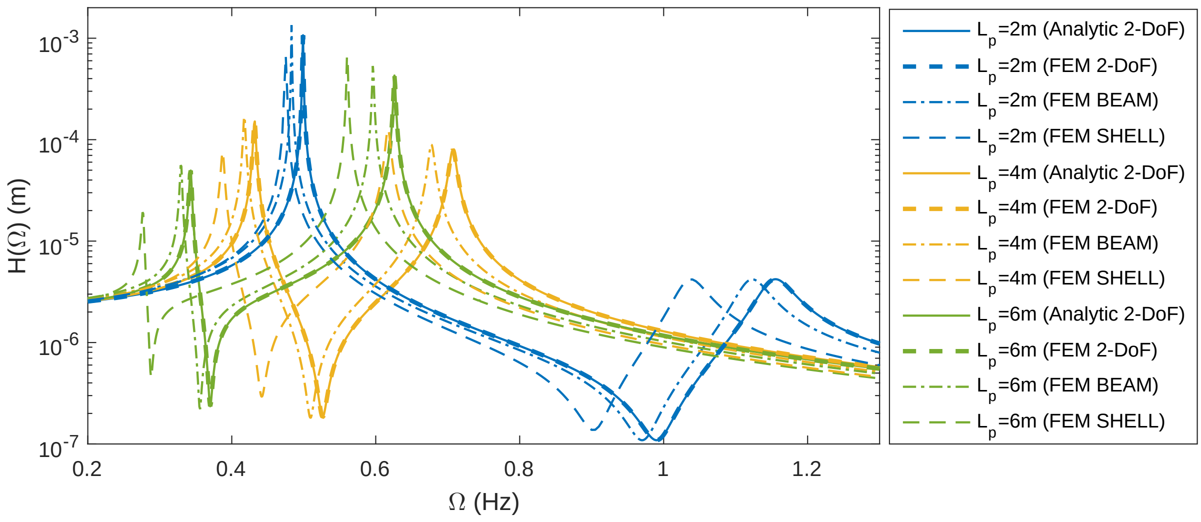

Figure 8: Frequency responses of the tower+pendulum for Analytical/FEM 2-Do , FEM BEAM, and FEM SHELL

models. The relative error for the FEM SHELL becomes very significantly reaching values greater than 30% for $L_p > 9m$ in the first mode and errors around 10% for the second mode.

The Table 1 shows values of the natural frequencies for the firsts and seconds modes for all models (in function of L_p), with its respective relative errors.

Table 1: Natural frequencies for the first and second mode of the FEM 2-DoF, FEM BEAM and FEM SHELL models for different L_p

$\omega_n(Hz)$	L_p (m)							
	2	**3**	**4**	**5**	**6**	**7**	**8**	**9**
1^{st} **mode**								
2-DoF	$0,499$	$0,473$	$0,432$	$0,385$	$0,343$	$0,308$	$0,279$	$0,256$
FEM BEAM	$0,483$	$0,458$	$0,417$	$0,371$	$0,329$	$0,295$	$0,267$	$0,245$
error % (BEAM)	$3,21$	$3,17$	$3,47$	$3,64$	$4,08$	$4,22$	$4,30$	$4,30$
FEM SHELL	$0,475$	$0,445$	$0,387$	$0,325$	$0,276$	$0,235$	$0,205$	$0,180$
error % (BEAM)	$4,81$	$5,92$	$10,42$	$15,58$	$19,53$	$23,70$	$26,52$	$29,69$
2^{nd} **mode**								
2-DoF	$1,155$	$0,837$	$0,707$	$0,652$	$0,626$	$0,613$	$0,605$	$0,600$
FEM BEAM	$1,123$	$0,807$	$0,677$	$0,622$	$0,596$	$0,582$	$0,574$	$0,568$
erro % (BEAM)	$2,77$	$3,58$	$4,24$	$4,60$	$4,79$	$5,06$	$5,12$	$5,33$
FEM SHELL	$1,038$	$0,730$	$0,617$	$0,577$	$0,560$	$0,550$	$0,545$	$0,543$
error % (SHELL)	$10,13$	$12,78$	$12,73$	$11,50$	$10,54$	$10,28$	$9,92$	$9,50$

5.1 2-DoF → BEAM FRF approximation

We propose an approach of the 2-DoF to the FEM BEAM model. The first step is to obtain the FRFs excluding the Pendulum TMD. Therefore, we makes up a simulation of the tower for a 2-DoF model to an extreme case, making $M_p = 0,1kg$ e $L_p = 0,1m$ (Figure 9).

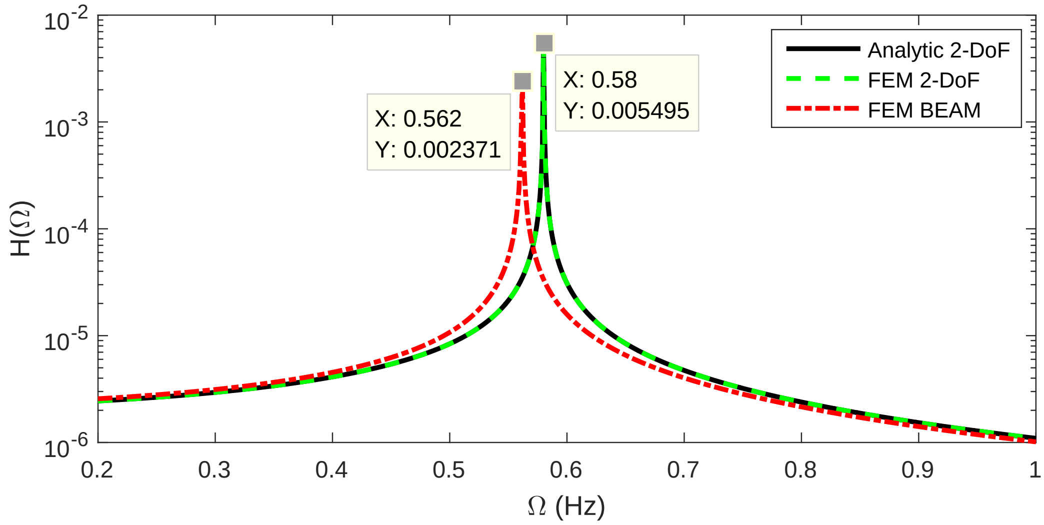

Figure 9: Extreme FRF case ($M_p = 0,1kg$**;** $L_p = 0,1m$) **for 2-DoF and FEM BEAM**

The difference between the resonance frequencies of the 2-DoF and FEM BEAM, for this extreme case, are calculated by (10).

$$\Omega_{corr} = \Omega_{2DoF} - \Omega_{BEAM} = 0,018Hz \tag{10}$$

where Ω_{corr} is the correction factor to approximate 2-DoF to an BEAM FEM model.

Figure 10 shows the correction made after applying the shift dislocation factor Ω_{corr} to the 2-DoF model.

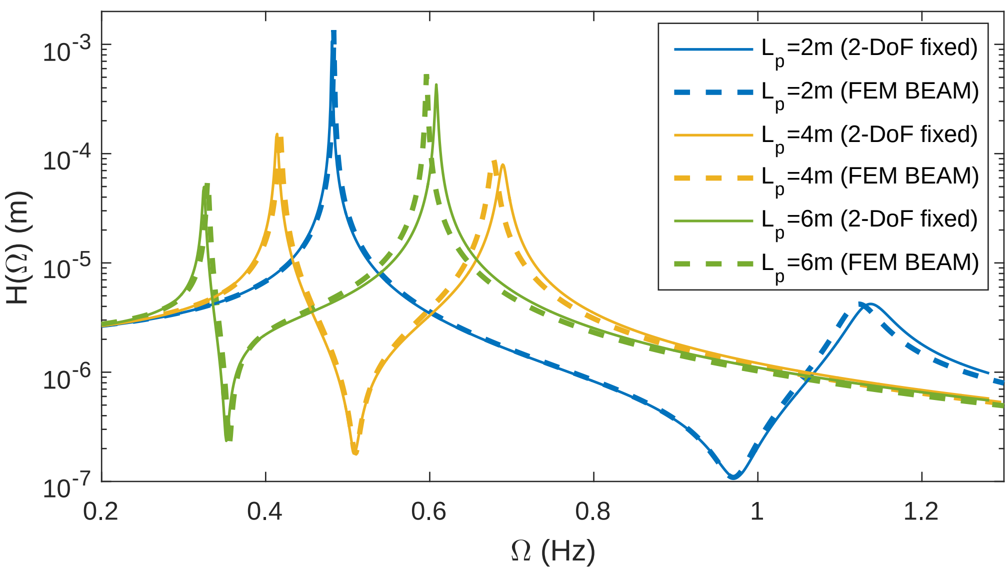

Figure 10: Frequency response of the 2-DoF fixed and FEM BEAM

Table 2 shows errors after application of the frequency correction Ω_{corr}. This correction reduces the relative error ($error \approx 1\%$).

Table 2: Natural frequencies for the first and second modes for the corrected 2-DoF and FEM BEAM for different lengths L_p

$\omega_n(Hz)$	L_p (m)		
	2	**4**	**6**
1^{st} **mode**			
2-DoF corr	$0,481$	$0,414$	$0,325$
FEM BEAM	$0,483$	$0,417$	$0,329$
error %	$0,41$	$0,72$	$1,22$
2^{nd} **mode**			
2-DoF corr	$1,137$	$0,689$	$0,608$
FEM BEAM	$1,123$	$0,677$	$0,596$
error %	$1,25$	$1,77$	$2,01$

6 Pendulum TMD Project

It's proposed a methodology project for the vibration absorber design based on the theory presented. A case study example is also showed.

6.1 Methodology

1^{st} step - Modal analysis of the tower

At this stage it's important to understand the dynamic behavior of the wind tower to be controlled. The modal analysis of the first resonance frequency and mode shape should be performed. The dynamic characteristics are reduced to a 2-DoF model.

2^{nd} step - Set the stiffness K_p and damping C_p

Damping C_p does not have direct influence on the behavior of the variables μ and L_p but only on the amplitude of frequency response $H_y(\omega)$ (Section 3.1). Thus the damping C_p is not a design decision factor, and may be selected arbitrarily according to availability.

For lower stiffness values, lower response amplitudes are obtained. So it's proposed a selection of a smaller stiffness K_p.

3^{rd} step - (L_p;μ) selection through optimization curves

The (L_p;μ) values are selected by the regression power curves (Figure 7) with its respective K_p.

4^{th} **step -** $\Omega_{2-GdL} \rightarrow \Omega_{viga}$ **correction**

Using selected pendulum settings (C_p;K_p;L_p;μ), the correction Ω_{corr} (Eq. 10) is applied for the approximation of a Analytical 2-DoF to a BEAM FEM.

5^{th} **step - Comparison between 2-DoF fixed and FEM BEAM**

In this last step the 2-DoF fixed model is compared to the FEM BEAM.

6.2 Case study

This case study is based on the model design presented, therefore the dynamic behavior of the 1^{st} **step** is already defined (Fig. 5).

Applying 2^{nd} **step**, it's defined that the damping $C_p = 9024, 9Nms$ is known. The stiffness $K_p = 5, 00.10^5 N/m$ is selected.

For μ values below 0.1 we noticed a FRF behavior different of the expected in the FEM BEAM model. So in 3^{rd} **step**, the mass ratio $\mu = 0.1349kg$ is chosen. Figure 11 shows the selection process of the length $L_p \approx 7, 7m$ by the power regression curve for $K_p = 5, 00.10^5 N/m$.

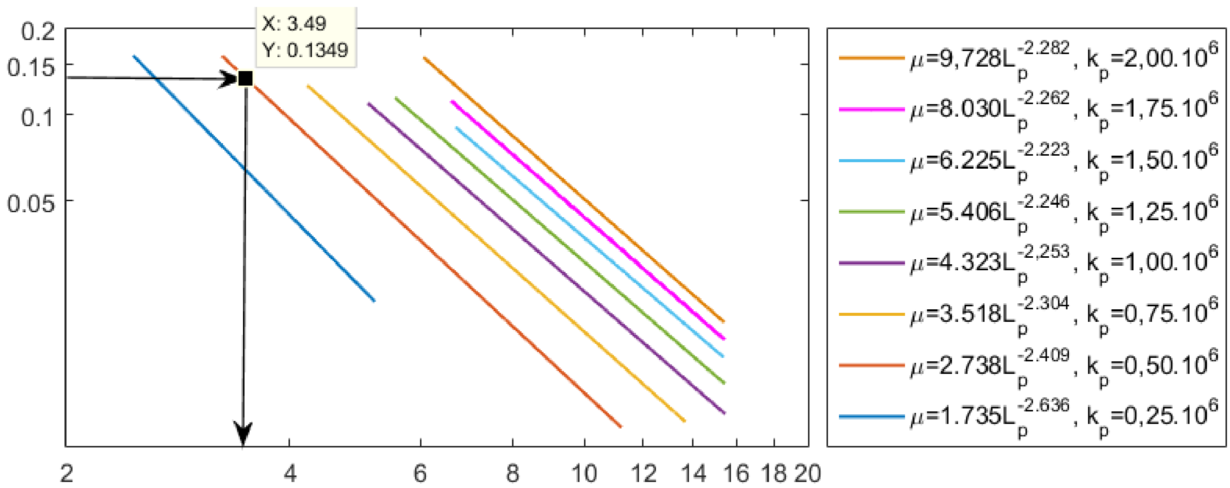

Figure 11: Optimum pendulum configuration in function of μ, L_p and K_p (N/m)

According of 4^{th} **step** we applies the Ω_{corr} correction. Then the 5^{th} **step** obtains the results of the Figure 12.

The expected results are obtained and the relative errors between the FEM BEAM and 2-DoF fixed models are 1.11% and 0.77% for the first and second resonance frequencies, respectively.

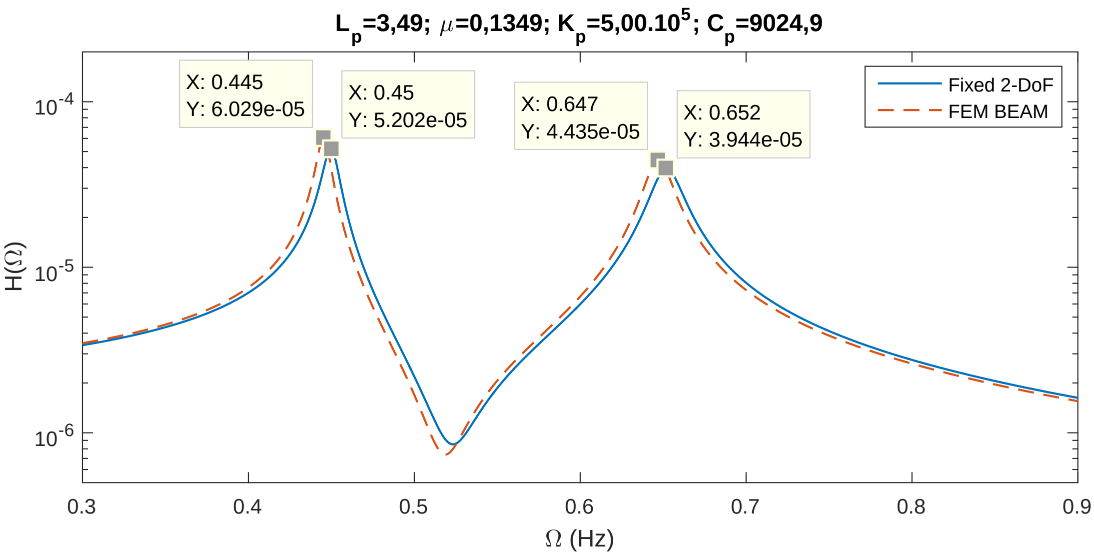

Figure 12: 2-DoF fixed FRF compared to the FEM BEAM model

7 Conclusions

The GA toolbox allows the identification of a geometric locus of the 2-DoF analytical solution of a Tower+Pendulum-TMD with have the optimum pendulum settings to absorb the wind tower vibration. An study of these response maps identifies the influence of the stiffness and damping of the pendulum through the response peaks of the tower. Many optimizations were made to obtain power regression curves in function of the stiffness with allows the selection of optimum pendulum TMD configurations. A methodology was proposed to select these configurations and an study case was discussed comparing the results with FEM models. For future studies we can create another fitness functions that analyzes the FRFs of the dynamic behavior of the tower.

ACKNOWLEDGEMENTS

The authors greetings CNPq (Brazilian Scientific Conseil) and MCTI (Industrial, Science and Technology Ministry) by financial support (Process 406895/2013-9) referent to scientific project edital MCTI/CNPq 74/2013 "Capacitação laboratorial e formação de recursos humanos em Energia Eólica (Linha 1)".

Bibliography

Avila, S. M., Morais, M. V. G., Barcelos, M., Shzu, M. A. M., & Silva, R. C. (2009). *Vibration Control of the set tower and wind turbine under the wind influence*. 20th International Congress of Mechanical Engineering, COBEM 2009, Gramado, RS, Brazil. pages 2, 5

Avila, S. M., Shzu, M. A. M., Pereira, W. M., Santos, L. S., Morais, M. V. G., & Prado, Z. J. G. (2016). *Numerical Modeling of the Dynamic Behavior of a Wind Turbine Tower*. Article in Advances in Vibration Engineering. pages 2, 9

Colherinhas, G. B., Morais, M. V. G., Shzu, M. A. M., & Ávila, S. M. (2015a). *Genetic Optimization of Tower Vibrations with Pendulum TMD*. CILAMCE 2015, XXXVI Ibero-Latin American Confress on Computational Methods in Engineering. pages 2

Colherinhas, G. B., Shzu, M. A. M., Ávila, S. M., & Morais, M. V. G. (2015b). *Genetic Optimization of Tower Vibrations with Pendulum TMD*. COMPDYN 2015, 5th ECCOMAS Thematic Conference on Computational Methods in Structural Dynamics and Earthquake Engineering. pages 2

Lackner, M. A., & Rotea, M. A. (2011). *Passive structural control of offshore wind turbines*, vol. 14. John Wiley & Sons, Ltd. pages 2

Meirovitch, L. (1967). *Analytical methods in vibrations*. Macmillan series in advanced mathematics and theoretical physics. Macmillan.
URL `https://books.google.com.br/books?id=sf1QAAAAMAAJ` pages 3

Morais, M. V. G., Barcelos, M., Ávila, S. M., Shzu, M. A. M., & de C. Silva, R. (2009). *Dynamic ehavior analysis of Wind Turbine towers*. Congreso de Métodos Numéricos en Ingeniería, Barcelona, 29 junio al 2 de julio, SEMNI, España. pages 2, 3

Murtagh, P. J., Basu, B., & Broderick, B. M. (2004). *Simple models for natural frequencies and mode shapes of towers supporting utilities*. pages 5

Nigdeli, S. M., & Bekdaş, G. (2016). *Optimum tuned mass damper design in frequency domain for structures*. pages 2

Shzu, M. A. M., Morais, M. V. G., del Prado, Z. J. G., & Ávila, S. M. (2015). *Finite Element Analysis of a Wind Turbine Tower with a Pendulum Tuned Mass Damper*. DINAME 2015 - XVII International Symposium on Dynamic Problems of Mechanics, ABCM, RN, Brazil, Frebruary 22-27. pages 2, 5, 9

Soong, T., & Dargush, G. (1997). *Passive Energy Dissipation Systems in Structural Engineering*.

Wiley.
URL `https://books.google.com.br/books?id=OxBmQgAACAAJ` pages 2, 4

Stewart, G. M., & Lackner, M. A. (2014). *The impact of passive tuned mass dampers and wind–wave misalignment on offshore wind turbine loads*, vol. 73.
URL `http://www.sciencedirect.com/science/book/pii/S0141029614002673` pages 2

Zuluaga, A. L. (2007). *Controle de vibrações em edifícios submetidos à ação de cargas dinâmicas utilizando amortecedor de massa sintonizado na forma de pêendulo*. Master's dissertation in Structures and Civil Construction, Universidade de Brasília. pages 4